NEOPLASIA
www.neoplasia.com

Volume 11 Number 8 August 2009 pp. 753–762 753

Mdm2 Deficiency Suppresses MYCN-Driven Neuroblastoma Tumorigenesis *In Vivo*[1]

Zaowen Chen*[,2], Yunfu Lin[†,2], Eveline Barbieri*, Sue Burlingame*, John Hicks[‡], Andrew Ludwig* and Jason M. Shohet*

*Texas Children's Cancer Center and Center for Cell and Gene Therapy, Baylor College of Medicine, Houston, TX 77030, USA; [†]Department of Biochemistry and Molecular Biology, Baylor College of Medicine, Houston, TX 77030, USA; [‡]Department of Pathology, Baylor College of Medicine, Houston, TX 77030, USA

Abstract

Neuroblastoma is derived from neural crest precursor components of the peripheral sympathetic nervous system and accounts for more than 15% of all pediatric cancer deaths. A clearer understanding of the molecular basis of neuroblastoma is required for novel therapeutic approaches to improve morbidity and mortality. Neuroblastoma is uniformly p53 wild type at diagnosis and must overcome p53-mediated tumor suppression during pathogenesis. Amplification of the *MYCN* oncogene correlates with the most clinically aggressive form of the cancer, and MDM2, a primary inhibitor of the p53 tumor suppressor, is a direct transcriptional target of, and positively regulated by, both MYCN and MYCC. We hypothesize that MDM2 contributes to MYCN-driven tumorigenesis helping to ameliorate p53-dependent apoptotic oncogenic stress during tumor initiation and progression. To study the interaction of MYCN and MDM2, we generated an Mdm2 haploinsufficient transgenic animal model of neuroblastoma. In *Mdm2*$^{+/-}$ *MYCN* transgenics, tumor latency and animal survival are remarkably extended, whereas tumor incidence and growth are reduced. Analysis of the Mdm2/p53 pathway reveals remarkable p53 stabilization counterbalanced by epigenetic silencing of the *p19*^{Arf} gene in the Mdm2 haploinsufficient tumors. In human neuroblastoma xenograft models, conditional small interfering RNA–mediated knockdown of MDM2 in cells expressing wild-type p53 dramatically suppresses tumor growth in a p53-dependent manner. In summary, we provided evidence for a crucial role for direct inhibition of p53 by MDM2 and suppression of the p19^{ARF}/p53 axis in neuroblastoma tumorigenesis, supporting the development of therapies targeting these pathways.

Neoplasia (2009) 11, 753–762

Introduction

Neuroblastoma is an aggressive neural crest–derived pediatric malignancy for which there has been little improvement in outcomes for the past decade. With less than 40% long-term survival for metastatic disease, it accounts for at least 15% of all pediatric cancer deaths despite intense treatment regimens combining high-dose chemotherapy, surgery, and radiation [1]. Improving neuroblastoma therapy will require an improved understanding of the molecular pathogenesis and pathophysiology of disease development and progression. Whereas the *MYCN* (*N-Myc*) oncogene has long been associated with malignant transformation in neuroblastoma [2], recent work demonstrates an important pathogenic role for *MYCC* (*C-Myc*) as well [3]. The p53 apoptotic mechanisms are intact in MYCN-positive neuroblastomas [4], and MDM2 inhibition leads to an immediate onset of apoptosis [5,6].

A crucial observation for neuroblastoma is that less than 2% of *de novo* cancers have mutated p53 [7,8], and its downstream effector

Address all correspondence to: Jason M. Shohet, Texas Children's Cancer Center Baylor College of Medicine, 1102 Bates St, Rm 750.03, Houston, TX 77030.
E-mail: jmshohet@texaschildrenshospital.org

[1]This work was supported by grants from the American Cancer Society (RSG 0720901), the Gilson-Longenbaugh Foundation, and the Hope Street Kids Foundation.
[2]These authors contribute equally.
Received 11 March 2009; Revised 26 April 2009; Accepted 30 April 2009

DOI 10.1593/neo.09466

pathways leading to cell cycle arrest and apoptosis are functionally active in most neuroblastoma tumors and cell lines [4,9–11]. This suggests that inhibition of p53 activation upstream plays a critical role in neuroblastoma tumorigenesis and that therapeutic reversal of this inhibition should, in principle, lead to p53 activation and tumor death *in vivo* [6,12]. Several *in vitro* and *in vivo* studies of MYCN demonstrate that this oncogene promotes cellular proliferation, metastasis, and genomic instability while also activating p53-mediated apoptotic stress responses [13]. A deeper understanding of the mechanisms regulating the balance between proliferation and apoptosis in *MYC* oncogene stressed that cells will aid the rational design of better-targeted molecular therapies.

MYCN gene amplification remains the strongest negative prognostic marker in neuroblastoma conferring a particularly poor term survival [14–16]. *MYCN* is amplified (>10 copies per cell) in more than 25% of neuroblastomas and is associated with an extremely aggressive metastatic phenotype. Interestingly, in *MYCN* nonamplified tumors, the levels of *MYCN* transcript and MYCN protein do not correlate as well with outcome [16–18]. It is also now apparent that the *MYCC* gene is frequently overexpressed in cells with low MYCN levels, suggesting that a common MYC-dependent transcriptional profile contributes to the pathogenesis of this type of cancer [3]. Several studies demonstrate that *Myc* oncogenes activate and repress a large number of genes directly through protein/DNA interactions [19] and through deregulation of microRNA [20–22]. Yet, how MYCN and MYCC specifically act to overcome p53-dependent cell cycle regulation and apoptosis in neuroblastoma remains to be elucidated.

The neuroblastoma-specific tumorigenic influence of MYCN was confirmed in a transgenic mouse model that targets the expression of human MYCN to neural crest cells using the tyrosine hydroxylase promoter (pTH-MYCN) [23]. These mice develop neuroblastoma that is histologically and genetically very similar to aggressive undifferentiated human neuroblastoma [24]. Importantly, the mouse model of neuroblastoma faithfully recapitulates the p53 wild-type status, chemosensitivity, and p53-dependent apoptotic responses of human neuroblastoma [25,26]. We modified this model to assess how MDM2 haploinsufficiency alters MYCN-driven tumorigenesis.

Amplification of the *MDM2* gene occurs in approximately 10% of human tumors (>30% of primarily sarcomas) and 2% of neuroblastoma, usually without coincident p53 mutation [11,27,28]. Transgenic mice overexpressing Mdm2 develop a wide spectrum of cancer suggesting that high MDM2 levels can overcome p53 tumor suppressor activity [29]. In line with these observations, inhibition of MDM2 with a small molecule that blocks the MDM2/p53 interaction (Nutlin-3a) leads to the reactivation of p53 functions and rapid apoptosis in neuroblastoma and other cancer cells [5,6]. Furthermore, MYCN-driven transactivation of MDM2 seems to inhibit apoptotic responses in neuroblastoma cell lines and primary cultures [30], but this has not been tested *in vivo*. Based on the central role of *MYC* oncogenes in neuroblastoma tumorigenesis and the necessity of inhibiting wild-type p53 activity to prevent apoptosis, we hypothesized that MDM2-mediated suppression of p53 is a vital component of MYCN-driven tumor initiation and progression.

The tumor suppressor ARF, produced as an *a*lternative *r*eading *f*rame of the $p16^{INK4a}$ gene, is the second most commonly mutated tumor suppressor in human malignancies behind p53 [31–34]. In contrast to p53, which responds to a variety of stresses, ARF is primarily activated by oncogenic stress and acts to counteract the proliferative activity of oncogenes such as *MYC*. ARF is frequently inactivated by gene deletion or promoter methylation [35,36]. This leads to less ARF/MDM2 complexes and more MDM2 free to inhibit p53. In normal cells, p53 downregulates *ARF* gene expression, forming an autoregulatory feedback loop [37].

To test this hypothesis, we crossed the well-characterized pTH-*MYCN* transgenic model of neuroblastoma and the *Mdm2* haploinsufficient mouse model [38] and compared tumor latency and incidence in the resulting animals. We found that $Mdm2^{+/-}MYCN^{+/+}$ transgenics had markedly delayed tumor development and had a lower overall incidence of tumors, strongly implicating Mdm2-mediated blockade of p53 as an essential step in the pathogenesis of neuroblastoma. Analysis of the resulting tumors demonstrated high levels of p53 and dramatically decreased levels of Arf. We further confirmed the impact of MDM2 levels on neuroblastoma growth in xenograft models using conditional short hairpin RNA (shRNA)–mediated knockdown of MDM2. Based on our data, we propose that both MYCN-mediated activation of MDM2 and suppression of ARF contribute directly to the pathogenesis of neuroblastoma. Further work designing molecular targeted therapies that modulate these pathways should provide clinically effective novel therapeutic approaches for neuroblastoma.

Materials and Methods

Cell Lines and Cell Culture

The ZC21 and SJ9 conditional subclones were generated from human neuroblastoma cells IMR32 (American Type Culture Collection, Manassas, VA) or SJ3-12 (a gift from Dr. Dirk Geerts, University of Amsterdam, the Netherlands) by transfection with pSuperior (OligoEngine, Seattle, WA) plasmids containing 64-bp shRNA hairpin loop constructs cloned into its unique *Bgl*II and *Hin*dIII sites. The MDM2 messenger RNA (mRNA) sequence targeted with small interfering RNA (siRNA) was gccattgcttttgaagtta. The expression of shRNA is driven by an inducible (Tet-ON) H1 promoter, which is activated by the presence of doxycycline. After transfection, cells were grown under puromycin selection for 2 weeks. Single clones were isolated, expanded, and characterized for their cellular MDM2 levels 72 hours after doxycycline treatment. Cell lines ZC21 and SJ9, showing remarkably decreased level of MDM2 as determined by Western blot, were used for the xenograft study. All types of cells were incubated at 37°C with 5% CO_2 in RPMI 1640 medium, supplemented with 10% fetal bovine serum and 1% penicillin-streptomycin (Invitrogen, Carlsbad, CA) antibiotics.

Western Blot Analysis

Briefly, cell pellets or tissue pieces were lysed in ice-cold cell lysis buffer (50 mM HEPES, 0.5% NP-40, 250 mM NaCl, pH 7.5) for 20 minutes in the presence of proteinase inhibitor cocktail (Roche, Indianapolis, IN) and PMSF. Typically, 50 to 75 μg of proteins was separated by SDS-PAGE on 4% to 15% gradient gels, transferred to polyvinylidene difluoride membrane, and incubated with individual antibodies (p53, p21, and CypB [Santa Cruz Biotechnology, Santa Cruz, CA]; HDMx/Mdm4 and $p14^{ARF}$ [Bethyl Laboratories, Montgomery, TX]; MDM2, MYCN, and $p19^{ARF}$ [Calbiochem, San Diego, CA]; and actin [Sigma, St. Louis, MO]). Immunoblots were then visualized by using enhanced chemiluminescence kit (GE Healthcare, Piscataway, NJ).

The protein mass of each band in Western blot was quantitatively measured using Usi-Scan-IT program (Silk Scientific, Inc., Orem, UT).

The relative amount of protein was calculated, after being divided by the quantitative mass of loading control proteins (β-actin or cyclophilin B) on the same lane.

Polymerase Chain Reaction and Reverse Transcription–Polymerase Chain Reaction

For real-time polymerase chain reaction (PCR), 100 ng of genomic DNA per reaction was assayed using the SYBR Green PCR kit (Qiagen, Valencia, CA). Results were normalized to the concentration of β-actin DNA and glyceraldehyde 3-phosphate dehydrogenase (GAPDH). Conditions for real-time PCR were 95°C for 15 minutes, followed by 45 cycles of 94°C for 15 seconds, 50°C for 30 seconds, and 72°C for 30 seconds. For reverse transcription (RT)–PCR, 50 ng of cellular total RNA was amplified with RT-PCR kit (Qiagen). For real-time RT-PCR, 50 ng of total RNA per reaction was assayed using the SYBR Green RT-PCR kit (Qiagen). Conditions for real-time RT-PCR were 50°C for 30 minutes, 95°C for 15 minutes, followed by 45 cycles of 94°C for 15 seconds, 50°C for 30 seconds, and 72°C for 30 seconds. The relative levels of mRNA and DNA were calculated by comparing number of cycles at which the PCR products became detectable above the basal threshold. The sequences of all PCR primers are listed in Table 1.

Table 1. Polymerase Chain Reaction Primers Used in This Study.

Target Gene	Primers	Purposes
Mdm2	ATCTGAGAGCTCGTGCCCTTCG TGTGGCTGGAGCATGGGTATTG GGCGGAAAGAACCAGCTGGGGC	Genotyping
MYCN	TGGAAAGCTTCTTATTGGTAGAAACAA AGGGATCCTTTCCGCCCCGTTCGTTTTAA	Genotyping
MYCN	CGACCACAAGGCCCTCAGTA CAGCCTTGGTGTTGGAGGAG	Genomic qPCR
β-actin (mouse)	TGCGTCTGGACTTGGCTG TAGCCACGCTCGGTCAGG	Genomic qPCR
p21 (mouse)	CCTGACAGATTTCTATCACTCCA CAGGCAGCGTATATCAGGAG	qRT-PCR
Mdm2	CTCTGGACTCGGAAGATTACAGCC CCTGTCTGATAGACTGTGACCCG	qRT-PCR
$p19^{Arf}$	GTCACAGTGAGGCCGCCGCTGA TGGGCGTGCTTGAGCTGAAGCTA	qRT-PCR
p53 (mouse)	TCTGGGACAGCCAAGTCTGT GGAGTCTTCCAGTGTCATGA	qRT-PCR
Mdm4	TGAGACCGTGTCAGAGCAATTAGG TCCACGTCAGTATCATCGCTCAAG	qRT-PCR
Gapdh	TCACCACCATGGAGAAGGC GCTAAGCAGTTGGTGGTGC	qRT-PCR

Mice Breeding

Mice were handled in accordance with an approved protocol from the Animal Research Committee of Baylor College of Medicine. $Mdm2^{+/-}$ mice (C57b strain; Dr. Lozano, MD Anderson Cancer Center) were first backcrossed for seven generations with wild-type 129/Svj mice to gain MDM2 heterozygous mice with 129/Svj strain ($Mdm2^{+/-}MYC^{-/-}$). The neuroblastoma model is highly strain-dependent, and to ensure equivalent comparisons, $Mdm2^{+/-}$ and $Mdm2^{+/+}$ mice were all derived from the same founding mice and littermates used for all analyses. For genotyping PCR, tail DNA was prepared using DNeasy kit (Qiagen) and genotyping for MDM2 performed as previously published [38]. MYCN heterozygosity or homozygosity was confirmed by quantitative PCR (qPCR) for the human pTH-MYCN transgene using the following primers.

Implantation of Neuroblastoma Xenograft

Five million ZC21 or SJ9 cells were resuspended together with 100 μl of Matrigel (BD Biosciences, San Jose, CA) and injected subcutaneously in 4-week-old severe combined immunodeficient (SCID) mice (Jackson Laboratory, Bar Harbor, ME) with mixed gender. One week after injection, mice were separated into two groups that were fed with drinking water either containing 2 mg/ml of doxycycline or not. Fresh water with or without doxycycline was served to the mice once every 2 days until the experiments were complete. The sizes of tumors in each mouse were measured daily starting from 10 days after cell injection. The data were plotted using Kaplan-Meier method to analyze the tumor growth.

Results

Mdm2 Deficiency Extends the Tumor Latency and Decreases Incidence in MYCN Transgenic Mice

To investigate the role of Mdm2 in neuroblastoma pathogenesis *in vivo*, we generated $MYCN^{+/+}$ transgenic mice (carrying two copies of the targeted transgene) with either wild-type $Mdm2^{+/+}$ or a heterozygous knockout $Mdm2^{+/-}$. The strategy for animal breeding is shown in Figure 1*A*. In pTH-MYCN transgenics, the human *MYCN* gene is driven by the tyrosine hydroxylase promoter, which is active in migrating cells of neural crest during early development and in the resulting peripheral sympathetic nervous tissue from which neuroblastoma arises [39]. *pTH-MYCN* transgenic mouse ($MYCN^{+/+}$, 129/Svj strain) spontaneously develops neuroblastoma in a MYCN dose-dependent manner [40,41]. Both cohorts contain two copies of human *MYCN* gene, express elevated levels of MYCN in neural crest precursors and developing sympathetic ganglia [23], and are expected to develop tumors efficiently, permitting us to study the role of Mdm2 on MYCN-driven tumors by comparing the two cohorts. Consistent with previous studies [38,42], we found no difference in animal weights, activity, oral intake, or fertility between cohorts. As expected, both $Mdm2^{+/+}$ and $Mdm2^{+/-}$ mice developed large abdominal neuroblastomas. Tumors from both groups had an aggressive undifferentiated phenotype with indistinguishable histologic diagnosis, morphology, and fine structure containing neurosecretory granules (Figure 1, *B* and *C*; data not shown).

Overall, 110 $Mdm2^{+/-}$ and 117 $Mdm2^{+/+}$ mice were observed for up to 1 year. Because no mice died of tumors after 110 days, we present Kaplan-Meier survival analysis taken out to 200 days (Figure 3). Mice were monitored at least twice a week for tumor formation and changes in health status. Mice were killed within 10 days of the detection of tumors to be examined in accordance with our institutional review board–approved animal protocol. Figure 2*A* illustrates the statistically significant differences in cumulative survival probabilities between $Mdm2^{+/-}$ and $Mdm2^{+/+}$ mice (as analyzed by Mantel-Cox and Wilcoxon methods). We found a dramatic difference in the median survival time (defined as time of sacrifice), which is closely correlated with tumor latency because these tumors, once fully established, are rapidly fatal. For $Mdm2^{+/+}$ mice, median latency was 55 days (95% confidence intervals [CI], 52-57 days), and for $Mdm2^{+/-}$ mice, tumor latency was 74 days (95% CI, 72-81 days; $P < .001$). Thus, the mean time to tumor onset was delayed approximately 20 days (38%) in the Mdm2 haploinsufficient mice, supporting our contention that Mdm2-mediated suppression of p53 is a rate-limiting step in MYCN-driven neuroblastoma tumorigenesis.

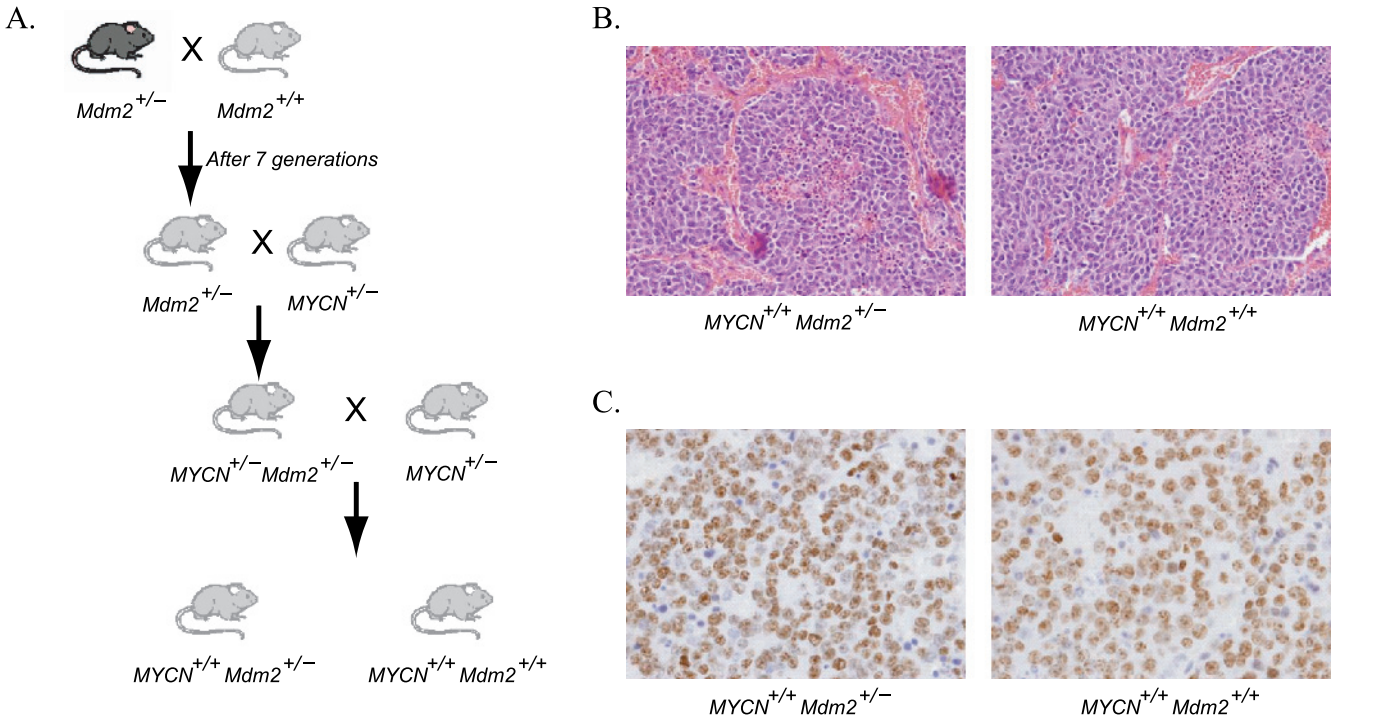

Figure 1. Generation of compound transgenic animals. (A) Breeding scheme used to generate matched sibling cohorts of Mdm2 haploinsufficient and Mdm2 wild-type mice with the homozygous human *MYCN* transgene in Svj-129 mice. The haploinsufficient mice were obtained from Dr. Lozano (MD Anderson Cancer Center) and backcrossed a minimum of seven generations into Svj-129 mice and then bred into the pTH-MYCN transgenic strain to obtain both $Mdm2^{+/-}$ and $Mdm2^{+/+}/MYCN^{+/+}$ compound transgenic mice. (B) Hematoxylin/eosin staining of both $Mdm2^{+/-}$ and $Mdm2^{+/+}$ tumors shows an aggressive undifferentiated histologic finding. (C) Tumors in both $Mdm2^{+/-}$ and $Mdm2^{+/+}$ were highly proliferative, and no differences in Ki-67 staining could be detected.

Overall, the MYCN transgenic mice wild type for Mdm2 had a very high incidence of tumors with 94% (110/117) of mice developing tumors, in line with previously published studies of the pTH-MYCN tumor model in the Svj-129 background [23,24]. However, the Mdm2 haploinsufficient mice had a significantly lower incidence of 80% overall (88/110 total; $P < .001$). This difference was sex-dependent (Figure 2, *B* and *C*). Seventy-six percent of female $Mdm2^{+/-}$ mice (47/62 animals) developed tumors compared with 93% (55/58 animals) of female *Mdm2* wild-type mice ($P < .001$). For male mice, Mdm2 haploinsufficiency had an insignificant influence on overall tumor incidence, with 89% (43/48 animals) of the $Mdm2^{+/-}$ mice compared with 95% (55/59 animals) of the *Mdm2* wild-type mice developing tumors (*P* value not significant; Figure 2*B*). Further analysis of tumor latency according to sex revealed a trend toward increased latency in the male $Mdm2^{+/-}$ mice compared with the female $Mdm2^{+/-}$, but this was not significant by Cox regression analysis (Figure 2, *legend*). No sex-dependent difference in latency or incidence was seen in the *Mdm2* wild-type pTH-MYCN mice (data not shown). The significant decrease in tumorigenesis in the female Mdm2-deficient mice may be secondary to interaction between MDM2 and the estrogen-dependent signaling in these mice (Discussion).

Because a major role of MDM2 is inhibition of p53 activity, it is possible that the delay to tumor formation and the reduced incidence reflect the need for additional genetic events to overcome increased p53-mediated tumor suppression. Mutations or deletion of the *p53* gene is exceptionally rare in primary human neuroblastoma, although there is an increased frequency of p53 mutations in relapsed tumors [7,43]. Because decreased Mdm2 and increased baseline p53 levels could lead to selective pressure to mutate p53 during tumorigenesis, we analyzed the sequences of p53 complementary DNA in a representative sample of tumors. Sequence data from 15 $Mdm2^{+/-}$ and 8 $Mdm2^{+/+}$ tumors revealed only wild-type p53 (data not shown), consistent with the almost complete absence of p53 mutations found in primary human neuroblastomas [8].

Mdm2 Deficiency Alters p53 Regulation and Activity in Neuroblastoma

The data shown in the previous section suggest that Mdm2 is critical for the development of MYCN-driven tumors and that a 50% decrease in Mdm2 significantly alters tumorigenesis. In cultured neuroblastoma cells, siRNA-mediated knockdown of MDM2 leads to a significant increase of p53 and sensitization to apoptotic stress [30]. To better understand the regulation of p53 and related proteins in $Mdm2^{+/-}$ and $Mdm2^{+/+}$ tumors, we performed semiquantitative Western blot and qRT-PCR analysis of Mdm2, p53, p21, Mdm4, $p19^{Arf}$, and MYCN in 12 tumors from each cohort, as shown in Figure 3, *A–C*. As expected, Mdm2 mRNA and protein levels are reduced to approximately 50% of wild type in the *Mdm2* haploinsufficient mice. Western blots demonstrate that p53 protein levels are remarkably higher in $Mdm2^{+/-}$ tumors, whereas the mRNA levels do not differ. This is consistent with decreased Mdm2-mediated ubiquitination of p53 and relative stabilization of the protein compared with $Mdm2^{+/+}$ tumors.

A primary transcriptional target of p53 is $p21^{CIP1/WAF1}$, which encodes the cyclin-dependent kinase inhibitor, p21, a central cell cycle regulator. Consistent with observations of increased p53 protein and

presumably its transcriptional activities, the average *p21* mRNA in *Mdm2*$^{+/-}$ tumors was approximately 80% higher than that in *Mdm2*$^{+/+}$. However, a trend toward decreased p21 protein levels is observed in *Mdm2*$^{+/-}$ tumors, suggesting that p21 protein is destabilized in these tumors. Interestingly, it has been shown that Mdm2 can inhibit p21 by promoting its ubiquitin-dependent and -independent proteosomal degradation [44,45]. However, decreased p21 protein levels would not be expected to correlate with decreased Mdm2 levels in *Mdm2*$^{+/-}$ mice, and an alternative mechanism for p21 protein reduction is likely invoked in this cohort.

We also analyzed levels of Mdm4 (also termed MdmX), a homolog of Mdm2 with overlapping and distinct regulatory effects on p53 [46]. The binding of Mdm4 to p53 at its N-terminal transactivation domain suppresses its transactivation activity [47], and Mdm4 has potent cell cycle effects independent of Mdm2 [48]. Although a trend toward decreased levels of Mdm4 can be seen, no significant change in Mdm4 protein or mRNA levels were detected. This suggests that Mdm4 levels do not compensate for low Mdm2 levels in *Mdm2*$^{+/-}$ tumors.

p19^{Arf} *Is Transcriptionally Repressed in Mdm2 Haploinsufficient Tumors*

The *p19*^{Arf} protein product Arf binds to and inactivates Mdm2 leading to the stabilization of p53 and subsequent apoptosis. Arf has both p53-dependent and p53-independent functions [31], and it has been shown to specifically bind to both human and mouse MYCC [49] and MYCN [50], inhibiting Myc transcriptional activity

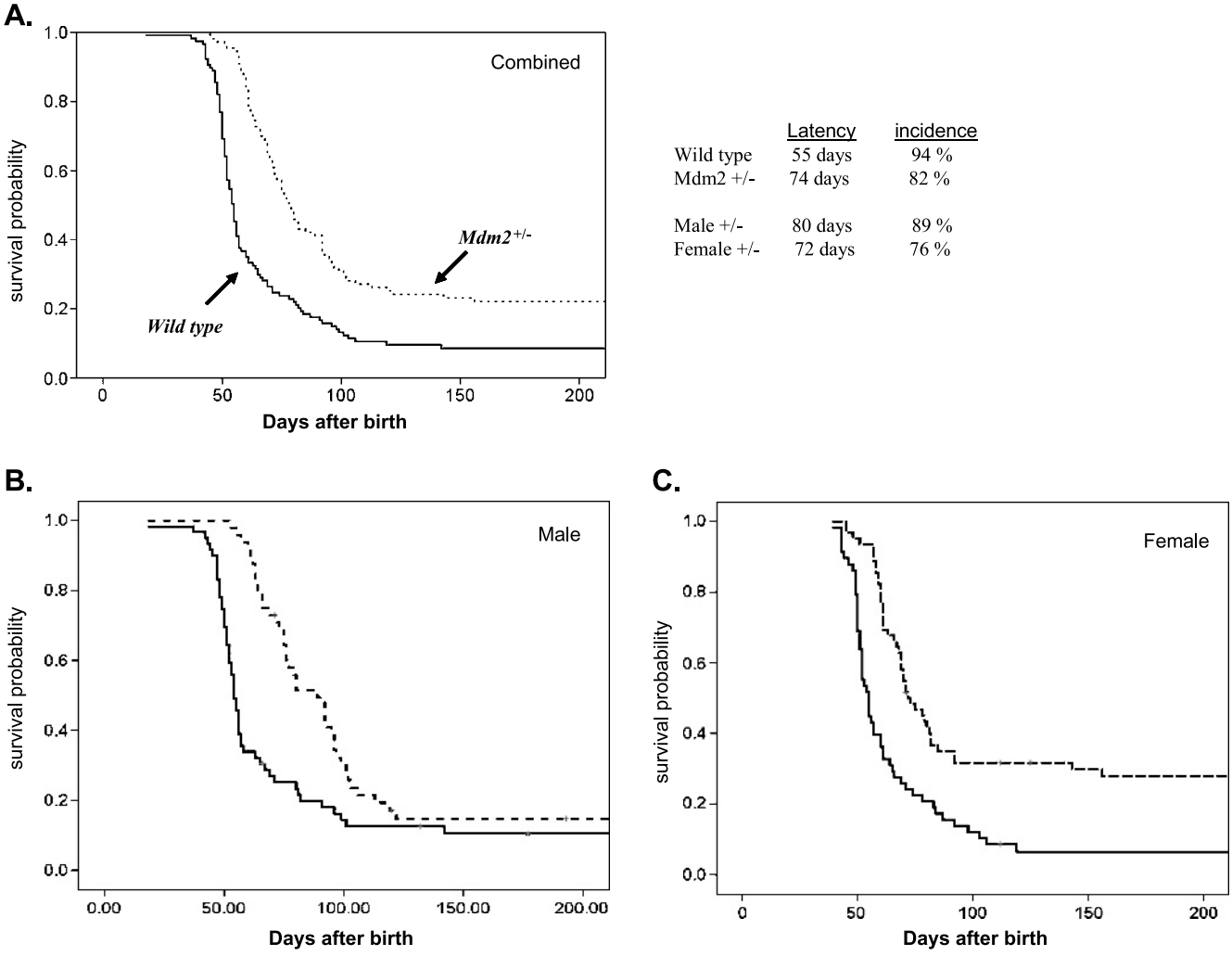

	Latency	incidence
Wild type	55 days	94 %
Mdm2 +/-	74 days	82 %
Male +/-	80 days	89 %
Female +/-	72 days	76 %

Figure 2. Tumor development in *Mdm2*$^{+/-}$ and *Mdm2*$^{+/+}$ pTH-MYCN transgenic mice. Kaplan-Meier survival probability curves plotted for *Mdm2*$^{+/+}$*/MYCN* (solid line) and *Mdm2*$^{+/-}$*/MYCN* (dashed line) transgenics at 200 days of observation. (A) Combined analysis of 110 *Mdm2*$^{+/-}$ and 117 *Mdm2*$^{+/+}$ mice shows a marked increase in median time to death (latency) and an overall decrease in tumor incidence ($P < .001$) consistent with the hypothesis that Mdm2 contributes directly to tumorigenesis in this model. (B) When analyzed according to sex, no difference in incidence was observed, but a significant increase in latency can be seen ($P < .001$). (C) For the female mice, an increase in latency but a pronounced decrease in incidence is now seen. No sex-dependent difference in tumor development was observed in the *Mdm2*$^{+/+}$ mice (latency 55 days [95% CI, 52-57 days]). Latency was 80 days (95% CI, 65-95 days) for the male *Mdm2*$^{+/-}$ mice and 71 days (95% CI, 63-78 days) for the female *Mdm2*$^{+/-}$ mice. Statistical analysis was performed with the SPSS software version (Gradware, Inc., Austin, TX), and both log-rank (Mantel-Cox) and Wilcoxon methods were applied. Comparisons of survival and latency between sexes for each genotype were performed by Cox regression analysis. Mouse totals: *Mdmd2*$^{+/-}$, 62 females and 48 males; *Mdm2*$^{+/+}$, 58 females and 59 males.

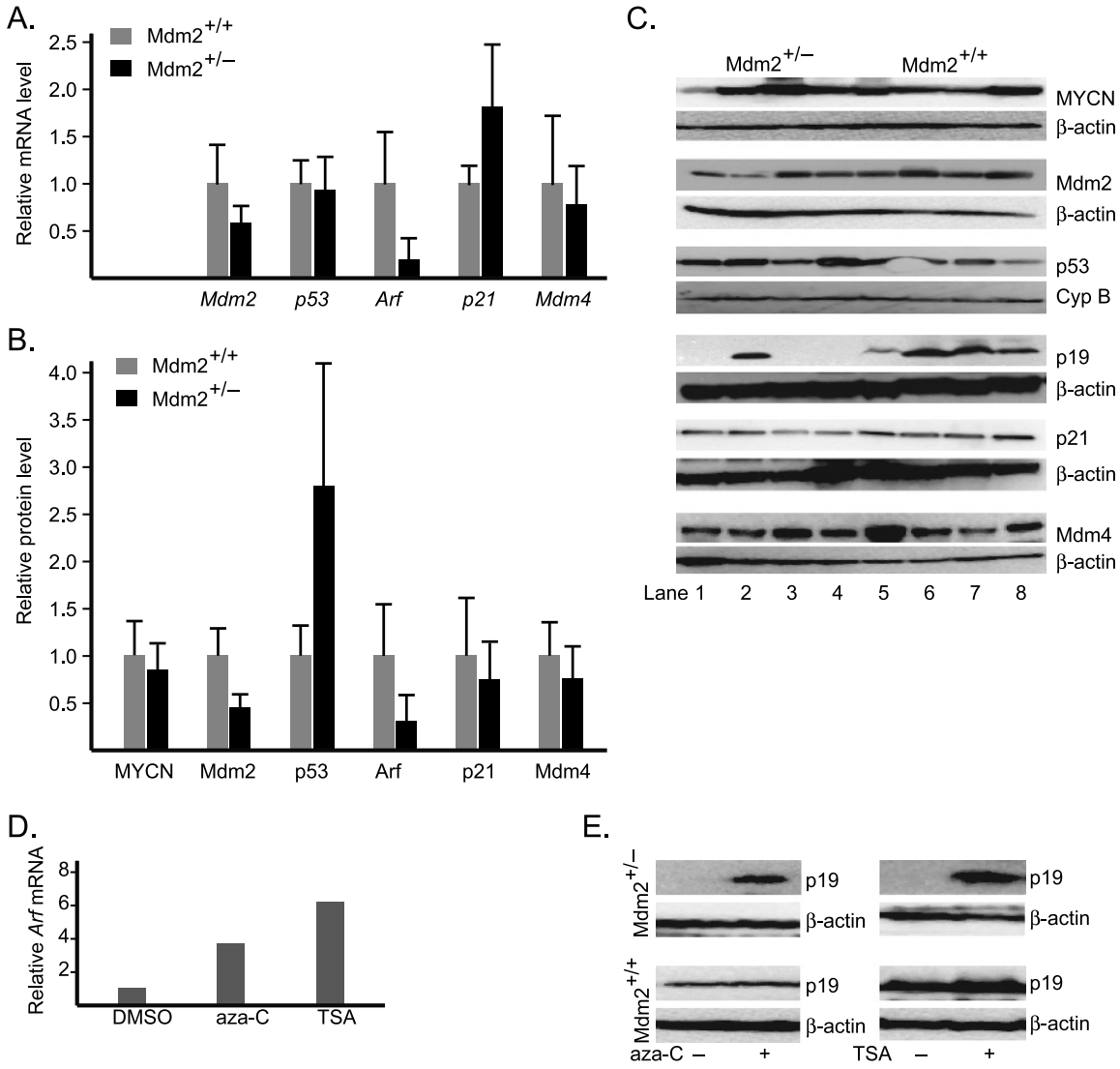

Figure 3. Gene expression patterns in tumors of *Mdm2*$^{+/-}$ and *Mdm2*$^{+/+}$ mice. (A) Comparison of relative transcript levels of *Mdm2*, *p53*, *Arf*, *p21*, and *Mdm4* genes. (B) Comparison of relative protein levels of MYCN, Mdm2, p53, p19^{Arf}, p21, and Mdm4. (C) Representative Western blot of MYCN, Mdm2, p53, p19^{Arf}, p21, and Mdm4. Analysis of protein levels in whole-cell extracts of tumors was assayed by immunoblot analysis using antibodies specific to each protein. Lanes 1 to 4 are for *Mdm2*$^{+/-}$, whereas lanes 5 to 8 are for *Mdm2*$^{+/+}$. Immunoblot analysis was also carried out for either β-actin or cyclophilin B as loading control. (D and E) There is re-expression of *Arf* gene in *Mdm2*$^{+/-}$ tumor cells after treatment with aza-C or trichostatin A (TSA), as shown by the increase of *Arf* transcript (D) and Arf protein (E). Student's *t* test was used for statistical analysis to evaluate significance.

and opposing the proliferative signals from oncogenes [51]. We therefore sought to determine Arf expression in both cohorts of mice.

Initially, we observed a striking lack of Arf expression at the protein level in most *Mdm2*$^{+/-}$ tumors and high expression in most *Mdm2*$^{+/+}$ tumors (Figure 3*B*), consistent with their corresponding levels of *Arf* mRNA (Figure 3*A*). The *p19*^{Arf} locus was not deleted as confirmed by quantitative genomic PCR (data not shown), suggesting an epigenetic mechanism for decreased Arf expression in the *Mdm2*$^{+/-}$ tumors. To test it, we isolated primary tumor cell lines from a *Mdm2*$^{+/-}$ tumor with no detectable Arf expression and a *Mdm2*$^{+/+}$ tumor with average expression. These transgenic mouse tumor lines were isolated by passaging tumors directly in mice and then in cell culture. We treated both lines with 1 μM of the demethylating agent 5′-aza-cytidine (aza-C) and the nonspecific histone deacetylase inhibitor trichostatin A. As shown in Figure 3, *D* and *E*, re-expression of Arf could be detected within 48 hours of treatment with either agent by both qRT-PCR and Western blot analysis.

As presented in Table 2, lack of Arf expression was commonly present in Mdm2 haploinsufficient *Mdm2*$^{+/-}$ tumors, but it was uncommonly observed in the Mdm2 wild-type *Mdm2*$^{+/+}$ tumors. In *Mdm2*$^{+/-}$ tumors, we have noted a statistically significant correlation with the level of Arf expression and the time to tumor development (Table 2), suggesting a key role of Arf on suppressing tumor growth when p53 levels are high. The exact role of Arf on inhibiting tumor growth is unclear; however, the increased tumor latency in *Mdm2*$^{+/-}$ may be due to the increased time required to silence the *p19*^{Arf} locus through DNA methylation or histone deacetylation events (Discussion). This protective effect of Arf is consistent with further decreased Mdm2 activity and increased p53 function in *Mdm2*$^{+/-}$ tumors.

Table 2. Relationship between p53 and $p19^{Arf}$ Levels with the Life Span of Mice from Cohorts A and B.

Mouse	p53 (%)	$p19^{Arf}$ (%)	Life Span (Days)
Mdm2$^{+/-}$			
A1	372	**57**	**122**
A2	198	**104**	**96**
A3	215	**55**	**95**
A4	593	**82**	**92**
A5	160	9	80
A6	569	3	79
A7	223	3	68
A8	264	12	63
A9	487	5	61
A10	275	11	60
A11	103	19	59
A12	305	13	45
Mdm2$^{+/+}$			
B1	79	138	80
B2	83	148	74
B3	120	36	71
B4	88	140	57
B5	110	56	56
B6	75	100	55
B7	161	193	54
B8	73	47	52
B9	124	59	51
B10	123	143	49
B11	104	28	48
B12	66	113	44

We determined the relative p53 and $p19^{Arf}$ protein levels in individual tumors by comparing the normalized values determined by Western blot analysis (with β-actin and cyclophilin B as loading controls) to the average level of each protein for all the Mdm2 wild-type tumors, which was arbitrarily defined as 100%. As shown, most *Mdm2*$^{+/-}$ tumors had markedly lower levels of $p19^{Arf}$ and markedly higher levels of p53 compared with the *Mdm2*$^{+/+}$ tumors. Signal levels were determined as described in the Materials and Methods section.

A clearly prolonged survival was noted in the tumors with relatively high $p19^{Arf}$ levels (shown in bold). This correlation was statistically validated using Cox regression analysis of time to sacrifice *versus* Arf level, which showed a correlation of $R = 0.07$ ($P < .012$) in the *Mdm2*$^{+/-}$ animals. No such correlation was evident in the Mdm2 wild-type tumors ($R = 0.18$, $P = .57$).

MDM2 Knockdown Suppresses Growth of Neuroblastoma Xenograft Formation

To further investigate the effect of MDM2 levels on human neuroblastoma growth *in vivo*, we used a xenograft model in SCID mice. We generated two human neuroblastoma cell lines, ZC21 and SJ9, expressing tet-inducible shRNA-targeting MDM2, constructed using IMR32 and SJ3-12 cells, respectively. IMR32 cells harbor wild-type p53, whereas SJ3-12 cells have a homozygous *p53* deletion removing a 21–amino acid region of the DNA binding domain of p53 leading to the loss of transactivation activity. In ZC21 cells, *MDM2* mRNA dropped to approximately 5% of the control level in 24 hours after doxycycline addition (data not shown), whereas the MDM2 protein decreased to approximately 50% and 10% in 48 and 72 hours, respectively (Figure 4*A*). Decrease of the MDM2 level was also observed in SJ9 cells (Figure 4*B*).

Fifteen age-matched SCID mice received subcutaneous injection with ZC21 cells, and tumor sizes were then monitored every 3 days. Eight test mice were given water containing 2 mg/ml doxycycline, whereas seven control mice were given plain water. As expected, the MDM2 level in the tumors from doxycycline-treated mice was substantially reduced compared with that from the untreated mice (Figure 4*C*). Tumor growth in these mice was individually tracked by serial measurements, and at 5 weeks, mice were killed, tumors were resected, and their sizes were measured. As shown in Figure 4*G*, mice treated with doxycycline developed smaller tumors than mice given with water only. In mice without doxycycline, the average tumor size was 1.1 cm^3, whereas mice treated with doxycycline developed tumors, with an average of 0.4 cm^3 ($P < .001$), indicating that the tumor growth was remarkably suppressed by MDM2 depletion.

As anticipated, MDM2 knockdown led to markedly elevated levels of p53 in the xenograft tumors ($P < .001$; Figure 4*E*), suggesting that a p53-dependent mechanism contributes to tumor growth suppression in this model. Interestingly, we saw a decrease in ARF protein levels in the MDM2 knockdown xenografts ($P < .005$), reflecting what was seen in the transgenic mouse model (Figure 4*E*). This may be due to the increased p53-dependent suppression of ARF [32]. To determine whether inhibition of xenograft growth was p53-dependent, we grew xenografts with the p53-mutant SJ9 conditional cell line that contains a 22–amino acid deletion within the p53 DNA binding domain (Figure 4*D*). In this line, MDM2 level was decreased by doxycycline treatment, whereas both p53 and ARF levels did not change (Figure 4*F*). Lack of p53 stabilization in response to Mdm2 silencing may be secondary to altered p53 turnover or ubiquitin-independent mechanisms of p53 regulation in this cell line. We saw no significant tumor suppression on MDM2 knockdown in the p53 mutant SJ9 line, which suggests that growth inhibition seen in the ZC21 cell line on MDM2 knockdown is p53-dependent. Taken together, these data demonstrate strong MDM2-dependent effects downstream of MYCN transactivation in both transgenic mouse tumors and human MYCN-amplified xenografts.

Discussion

In the data presented in this study, we provide the first *in vivo* evidence that MDM2 contributes to MYCN-driven tumorigenesis in neural crest–derived neuroblastoma with both Mdm2 haploinsufficient transgenic mice and human neuroblastoma xenografts in SCID mice using cell lines with shRNA-mediated conditional knockdown of MDM2. Both tumor latency and tumor incidence are significantly altered by the reduction in Mdm2 levels in the transgenic model. Importantly, tumor latency was also correlated with Arf levels in the p53 wild-type tumors. Molecular analyses comparing tumors from *Mdm2*$^{+/-}$ and *Mdm2*$^{+/+}$ reveal down-regulation of $p19^{Arf}$ expression at both the mRNA and protein level without gene deletion. Treatment of haploinsufficient tumor cells with the demethylating agent aza-C leads to rapid up-regulation of both $p19^{Arf}$ message and protein levels and stabilization of p53. In the next paragraphs, we discuss the potential function of Mdm2 as an effector of Myc-driven tumorigenesis in neuroblastoma through the disruption of the Arf/Mdm2/p53 regulatory network and p53-mediated tumor suppression. These results are placed in context of neuroblastic tumor initiation and progression in the pTH-MYCN transgenic mouse model of neuroblastoma.

We found a high rate of $p19^{Arf}$ suppression in *Mdm2*$^{+/-}$ tumors that are driven by MYCN and develop in the context of Mdm2 haploinsufficiency. Such suppression seems to be due to epigenetic silencing because the expression of $p19^{Arf}$ gene can be reactivated in culture tumor cells by epigenetic treatment. However, we have not identified the specific mechanism as to how $p19^{Arf}$ is regulated or identified at what point during tumorigenesis this event occurs. Nevertheless, our data support the hypothesis that reduction of ARF level is an important step for the development of p53 wild type MYCN-driven neuroblastoma in MDM2-deficient mice and in human tumor cell lines.

We also demonstrate a strong influence of sex on tumor incidence in the Mdm2 haploinsufficient mice with overall tumor rate, decreasing more than 18% in the female *Mdm2*$^{+/-}$ mice ($P < .001$). The

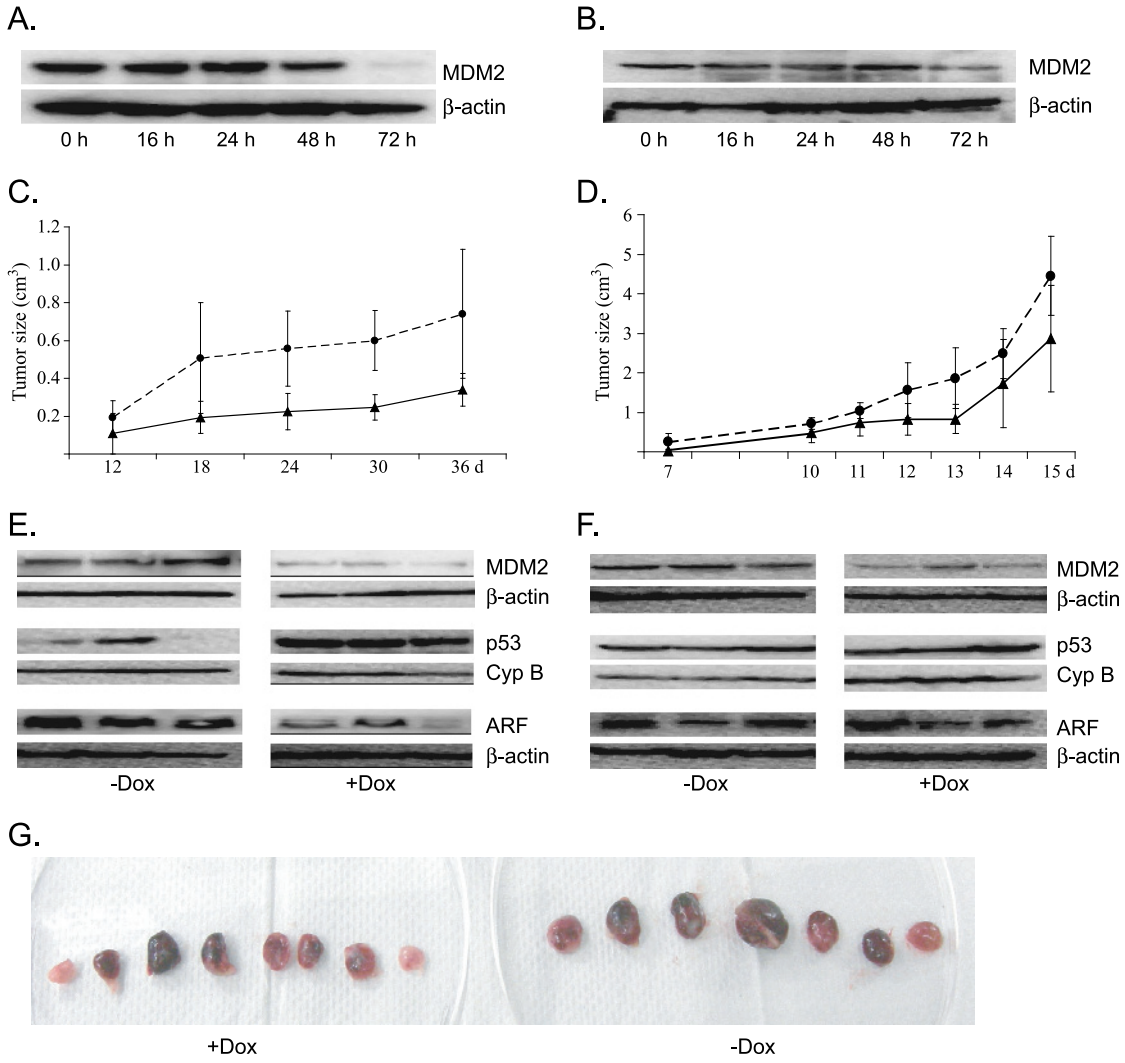

Figure 4. Xenograft tumor models of human neuroblastoma cell lines ZC21 and SJ9. (A and B) Change of MDM2 protein level after induction of shRNA-targeting *MDM2* gene in ZC21 (A) and SJ9 cells (B), respectively. As shown, MDM2 level is remarkably decreased 48 to 72 hours after induction of *MDM2*-specific shRNA with doxycycline. (C) Growth of xenograft tumors with the injection of ZC21 cells. After injection, mice were given water with or without 2 mg/ml doxycycline. The growth of xenograft tumor was significantly reduced by doxycycline feeding (solid line) compared with the tumor growth without doxycycline (dashed line). (D) Growth of tumor growth for SJ9. As shown, the growth of xenograft tumor with doxycycline feeding is slightly but nonsignificantly slower than control tumors. (E and F) Representative immunoblot for protein levels of MDM2, p53, and $p19^{ARF}$ from three xenograft tumors injected with ZC21 (E) or SJ9 cells (F), respectively. (G) Sizes of individual xenograft tumors injected with ZC21 cells. Student's *t* test was used for statistical analysis.

estrogen receptor α (ERα) interacts with Mdm2 and p53 and can inhibit Mdm2-mediated ubiquitination of p53 [52]. Subsequent increased p53 activity may be sufficient to further suppress tumorigenesis in female Mdm2 haploinsufficient mice. However, ERα may also act to increase Mdm2 levels indirectly and alter glucocorticoid receptor signaling [53], and Mdm2 can enhance ERα activity in breast cancer cells [54]. It is also possible that p53-independent functions of Mdm2 or mouse strain–specific effects account for the observed inhibition of tumorigenesis in the female mice. Neuroblastoma is almost exclusively found in premenarchal children, and clinical and mechanistic implications of these findings will require additional investigation.

Although the interactions of MDM2 and ARF have been well detailed [32], the observation of a direct interaction between MYCN and ARF adds an additional level of complexity to MYCN-driven tumorigenesis. Recently, it was shown that ARF can inhibit MYCN-mediated transcription through binding to both the MYCN DNA binding domain and its transactivation domains [50]. In our transgenic mice with only one functional *Mdm2* allele, it seems that low Mdm2 levels increase selective pressure to silence Arf during the process of malignant transformation/progression. There is little Arf suppression in the wild-type tumors. These results suggest that with normal (or high) Mdm2 levels, MYCN-driven transcription can overcome ARF-mediated suppression of MDM2, sufficiently repressing p53 for tumorigenesis to proceed. This model agrees with clinical data showing very rare epigenetic silencing or deletion of ARF in human neuroblastoma tumors [10,55] and also agrees with our data showing increased latency of the haploinsufficient $Mdm2^{+/-}$ tumors because more time and cell divisions may be needed for Arf suppression to occur *in vivo* (Figure 2).

Both MYCN and MYCC activate apoptosis and stimulate proliferation simultaneously in culture cells. How the neural crest–derived precursors of neuroblastoma respond to aberrant MYC activation clearly depends on direct MYC transcriptional targets and on indirect and parallel oncogenic stimuli. Recent studies comparing the sympathetic ganglia of pTH-MYCN and wild-type mice have shown that MYCN expression leads to the persistence of proliferative rests of neuroblasts and that this correlates with tumorigenesis in a *MYCN* gene dose-responsive manner [41]. The aberrant expression of MYCN (normally shut down early in embryogenesis) likely disrupts apoptosis and differentiation favoring the proliferation of these "neuroblast" cells. We demonstrate that haploinsufficiency of Mdm2 clearly prolongs tumor latency and decreases the incidence of tumor development in this same pTH-MYCN model. Lower levels of Mdm2 may weaken the oncogenic effect of MYCN in neuroblast precursors, increasing the requirement for additional genetic changes such as epigenetic silencing of ARF.

Similar findings to our data have been demonstrated in a different MYCC (C-Myc)-driven lymphoma model. In Eμ-*Myc* transgenic, overexpression of MYCC in B cells leads to B-cell lymphoma development, accompanied with frequent inactivation of p53 or ARF [56]. In this transgenic model, loss of one *Mdm2* allele increased p53-dependent B-cell apoptosis and reduced lymphomagenesis [57,58]. Suppression of Eμ-*Myc* lymphoma by Mdm2 deficiency was rescued by the inactivation of p53 or ARF [57,58], and lymphogenesis was accelerated by the overexpression of Mdm2 [59]. Whereas MYCN and MYCC have distinct expression profiles and transcriptional targets, our data in neuroblastoma (a neuronal crest–derived solid tumor) suggest a common requirement for p53 suppression downstream of *C-Myc* or *MYCN* oncogenes.

The clinical implications of these data are as follows. First, they strongly concur with two recent genetic analyses of neuroblastoma patient samples, suggesting that an activating single nucleotide polymorphism (SNP) in the human *MDM2* promoter, SNP($309_{T\ to\ G}$), correlates with a shorter time to relapse and a shorter time to death [60,61]. The SNP309 modifies an SP1 transcription factor binding site in the *MDM2* promoter, increasing affinity for SP1 and subsequent *MDM2* transcription and attenuated p53 responses [62]. Thus, elevated *MDM2* transcription seems to significantly alter the behavior of human neuroblastomas. Importantly, the incidence of homozygosity for the activating SNP (i.e., G/G allele) in neuroblastoma patients is twice that of controls [61], suggesting that elevated MDM2 levels contribute to neuroblastoma tumorigenesis. Second, after the induction of chemotherapy in the context of minimal residual disease, suppression of MDM2 activity with small-molecule inhibitors may prevent tumor regrowth and relapse, which is the primary cause of death in neuroblastoma. Previous *in vitro* studies demonstrate that neuroblastoma cells are extremely sensitive to MDM2 inhibitors, such as Nutlin-3a [5,6], which activate p53-directed apoptosis. This work lends further support to the therapeutic approach of using small-molecule inhibitors of MDM2 to "de-repress" p53 in several phases of treatment.

Acknowledgments

The authors thank the support and helpful discussions with Guillermina Lozano (MD Anderson) and Jeffery Rosen (Baylor College of Medicine). Statistical help was provided by E. Obrien Smith (Baylor College of Medicine).

References

[1] Brodeur GM (2003). Neuroblastoma: biological insights into a clinical enigma. *Nat Rev Cancer* **3**, 203–216.

[2] Small MB, Hay N, Schwab M, and Bishop JM (1987). Neoplastic transformation by the human gene N-*myc*. *Mol Cell Biol* **7**, 1638–1645.

[3] Westermann F, Muth D, Benner A, Bauer T, Henrich KO, Oberthur A, Brors B, Beissbarth T, Vandesompele J, Pattyn F, et al. (2008). Distinct transcriptional MYCN/c-MYC activities are associated with spontaneous regression or malignant progression in neuroblastomas. *Genome Biol* **9**, R150.

[4] Chen L, Malcolm AJ, Wood KM, Cole M, Variend S, Cullinane C, Pearson AD, Lunec J, and Tweddle DA (2007). p53 is nuclear and functional in both undifferentiated and differentiated neuroblastoma. *Cell Cycle* **6**, 2685–2696.

[5] Barbieri E, Mehta P, Chen Z, Zhang L, Slack A, Berg S, and Shohet JM (2006). MDM2 inhibition sensitizes neuroblastoma to chemotherapy-induced apoptotic cell death. *Mol Cancer Ther* **5**, 2358–2365.

[6] Van Maerken T, Speleman F, Vermeulen J, Lambertz I, De Clercq S, De Smet E, Yigit N, Coppens V, Philippe J, De Paepe A, et al. (2006). Small-molecule MDM2 antagonists as a new therapy concept for neuroblastoma. *Cancer Res* **66**, 9646–9655.

[7] Tweddle DA, Malcolm AJ, Bown N, Pearson AD, and Lunec J (2001). Evidence for the development of p53 mutations after cytotoxic therapy in a neuroblastoma cell line. *Cancer Res* **61**, 8–13.

[8] Vogan K, Bernstein M, Leclerc JM, Brisson L, Brossard J, Brodeur GM, Pelletier J, and Gros P (1993). Absence of *p53* gene mutations in primary neuroblastomas. *Cancer Res* **53**, 5269–5273.

[9] Keshelava N, Zuo JJ, Waidyaratne NS, Triche TJ, and Reynolds CP (2000). p53 mutations and loss of p53 function confer multidrug resistance in neuroblastoma. *Med Pediatr Oncol* **35**, 563–568.

[10] Tweddle DA, Malcolm AJ, Cole M, Pearson AD, and Lunec J (2001). p53 cellular localization and function in neuroblastoma: evidence for defective G(1) arrest despite WAF1 induction in MYCN-amplified cells. *Am J Pathol* **158**, 2067–2077.

[11] Tweddle DA, Pearson AD, Haber M, Norris MD, Xue C, Flemming C, and Lunec J (2003). The p53 pathway and its inactivation in neuroblastoma. *Cancer Lett* **197**, 93–98.

[12] Slack A and Shohet JM (2005). MDM2 as a critical effector of the *MYCN* oncogene in tumorigenesis. *Cell Cycle* **4**, 857–860.

[13] Ushmorov A, Hogarty MD, Liu X, Knauss H, Debatin KM, and Beltinger C (2008). N-*myc* augments death and attenuates protective effects of Bcl-2 in trophically stressed neuroblastoma cells. *Oncogene* **27**, 3424–3434.

[14] Maris JM, Hogarty MD, Bagatell R, and Cohn SL (2007). Neuroblastoma. *Lancet* **369**, 2106–2120.

[15] Mathew P, Valentine MB, Bowman LC, Rowe ST, Nash MB, Valentine VA, Cohn SL, Castleberry RP, Brodeur GM, and Look AT (2001). Detection of *MYCN* gene amplification in neuroblastoma by fluorescence *in situ* hybridization: a pediatric oncology group study. *Neoplasia* **3**, 105–109.

[16] Tang XX, Zhao H, Kung B, Kim DY, Hicks SL, Cohn SL, Cheung NK, Seeger RC, Evans AE, and Ikegaki N (2006). The MYCN enigma: significance of MYCN expression in neuroblastoma. *Cancer Res* **66**, 2826–2833.

[17] Cohn SL, London WB, Huang D, Katzenstein HM, Salwen HR, Reinhart T, Madafiglio J, Marshall GM, Norris MD, and Haber M (2000). MYCN expression is not prognostic of adverse outcome in advanced-stage neuroblastoma with nonamplified MYCN. *J Clin Oncol* **18**, 3604–3613.

[18] Cohn SL and Tweddle DA (2004). MYCN amplification remains prognostically strong 20 years after its "clinical debut". *Eur J Cancer* **40**, 2639–2642.

[19] Fernandez PC, Frank SR, Wang L, Schroeder M, Liu S, Greene J, Cocito A, and Amati B (2003). Genomic targets of the human c-Myc protein. *Genes Dev* **17**, 1115–1129.

[20] Chang TC, Yu D, Lee YS, Wentzel EA, Arking DE, West KM, Dang CV, Thomas-Tikhonenko A, and Mendell JT (2008). Widespread microRNA repression by Myc contributes to tumorigenesis. *Nat Genet* **40**, 43–50.

[21] Chen Y and Stallings RL (2007). Differential patterns of microRNA expression in neuroblastoma are correlated with prognosis, differentiation, and apoptosis. *Cancer Res* **67**, 976–983.

[22] Schulte JH, Horn S, Otto T, Samans B, Heukamp LC, Eilers UC, Krause M, Astrahantseff K, Klein-Hitpass L, Buettner R, et al. (2008). MYCN regulates oncogenic microRNAs in neuroblastoma. *Int J Cancer* **122**, 699–704.

[23] Weiss WA, Aldape K, Mohapatra G, Feuerstein BG, and Bishop JM (1997). Targeted expression of MYCN causes neuroblastoma in transgenic mice. *EMBO J* **16**, 2985–2995.

[24] Moore HC, Wood KM, Jackson MS, Lastowska MA, Hall D, Imrie H, Redfern CP, Lovat PE, Ponthan F, O'Toole K, et al. (2008). Histological profile of tumours from MYCN transgenic mice. *J Clin Pathol* **61**, 1098–1103.

[25] Cheng AJ, Cheng NC, Ford J, Smith J, Murray JE, Flemming C, Lastowska M, Jackson MS, Hackett CS, Weiss WA, et al. (2007). Cell lines from MYCN transgenic murine tumours reflect the molecular and biological characteristics of human neuroblastoma. *Eur J Cancer* **43**, 1467–1475.

[26] Chesler L, Goldenberg DD, Collins R, Grimmer M, Kim GE, Tihan T, Nguyen K, Yakovenko S, Matthay KK, and Weiss WA (2008). Chemotherapy-induced apoptosis in a transgenic model of neuroblastoma proceeds through p53 induction. *Neoplasia* **10**, 1268–1274.

[27] Corvi R, Savelyeva L, Breit S, Wenzel A, Handgretinger R, Barak J, Oren M, Amler L, and Schwab M (1995). Non-syntenic amplification of MDM2 and MYCN in human neuroblastoma. *Oncogene* **10**, 1081–1086.

[28] Momand J, Jung D, Wilczynski S, and Niland J (1998). The *MDM2* gene amplification database. *Nucleic Acids Res* **26**, 3453–3459.

[29] Jones SN, Hancock AR, Vogel H, Donehower LA, and Bradley A (1998). Overexpression of Mdm2 in mice reveals a p53-independent role for Mdm2 in tumorigenesis. *Proc Natl Acad Sci USA* **95**, 15608–15612.

[30] Slack A, Chen Z, Tonelli R, Pule M, Hunt L, Pession A, and Shohet JM (2005). The p53 regulatory gene *MDM2* is a direct transcriptional target of MYCN in neuroblastoma. *Proc Natl Acad Sci USA* **102**, 731–736.

[31] Sherr CJ (2001). The INK4a/ARF network in tumour suppression. *Nat Rev Mol Cell Biol* **2**, 731–737.

[32] Sherr CJ (2006). Divorcing ARF and p53: an unsettled case. *Nat Rev Cancer* **6**, 663–673.

[33] Zhang Y, Xiong Y, and Yarbrough WG (1998). ARF promotes MDM2 degradation and stabilizes p53: ARF-INK4a locus deletion impairs both the Rb and p53 tumor suppression pathways. *Cell* **92**, 725–734.

[34] Pomerantz J, Schreiber-Agus N, Liegeois NJ, Silverman A, Alland L, Chin L, Potes J, Chen K, Orlow I, Lee HW, et al. (1998). The Ink4a tumor suppressor gene product, p19Arf, interacts with MDM2 and neutralizes MDM2's inhibition of p53. *Cell* **92**, 713–723.

[35] Kim WY and Sharpless NE (2006). The regulation of INK4/ARF in cancer and aging. *Cell* **127**, 265–275.

[36] Esteller M (2002). CpG island hypermethylation and tumor suppressor genes: a booming present, a brighter future. *Oncogene* **21**, 5427–5440.

[37] Robertson KD and Jones PA (1998). The human ARF cell cycle regulatory gene promoter is a CpG island which can be silenced by DNA methylation and down-regulated by wild-type p53. *Mol Cell Biol* **18**, 6457–6473.

[38] Montes de Oca Luna R, Wagner DS, and Lozano G (1995). Rescue of early embryonic lethality in mdm2-deficient mice by deletion of p53. *Nature* **378**, 203–206.

[39] Banerjee SA, Hoppe P, Brilliant M, and Chikaraishi DM (1992). 5′ flanking sequences of the rat tyrosine hydroxylase gene target accurate tissue-specific, developmental, and transsynaptic expression in transgenic mice. *J Neurosci* **12**, 4460–4467.

[40] Chesler L, Goldenberg DD, Seales IT, Satchi-Fainaro R, Grimmer M, Collins R, Struett C, Nguyen KN, Kim G, Tihan T, et al. (2007). Malignant progression and blockade of angiogenesis in a murine transgenic model of neuroblastoma. *Cancer Res* **67**, 9435–9442.

[41] Hansford LM, Thomas WD, Keating JM, Burkhart CA, Peaston AE, Norris MD, Haber M, Armati PJ, Weiss WA, and Marshall GM (2004). Mechanisms of embryonal tumor initiation: distinct roles for MycN expression and MYCN amplification. *Proc Natl Acad Sci USA* **101**, 12664–12669.

[42] McMasters KM, Montes de Oca Luna R, Pena JR, and Lozano G (1996). mdm2 deletion does not alter growth characteristics of p53-deficient embryo fibroblasts. *Oncogene* **13**, 1731–1736.

[43] Carr J, Bell E, Pearson AD, Kees UR, Beris H, Lunec J, and Tweddle DA (2006). Increased frequency of aberrations in the p53/MDM2/p14(ARF) pathway in neuroblastoma cell lines established at relapse. *Cancer Res* **66**, 2138–2145.

[44] Jin Y, Lee H, Zeng SX, Dai MS, and Lu H (2003). MDM2 promotes $p21^{waf1/cip1}$ proteasomal turnover independently of ubiquitylation. *EMBO J* **22**, 6365–6377.

[45] Zhang Z, Wang H, Li M, Agrawal S, Chen X, and Zhang R (2004). MDM2 is a negative regulator of $p21^{WAF1/CIP1}$, independent of p53. *J Biol Chem* **279**, 16000–16006.

[46] Grier JD, Xiong S, Elizondo-Fraire AC, Parant JM, and Lozano G (2006). Tissue-specific differences of p53 inhibition by Mdm2 and Mdm4. *Mol Cell Biol* **26**, 192–198.

[47] Shvarts A, Steegenga WT, Riteco N, van Laar T, Dekker P, Bazuine M, van Ham RC, van der Houven van Oordt W, Hateboer G, van der Eb AJ, et al. (1996). MDMX: a novel p53-binding protein with some functional properties of MDM2. *EMBO J* **15**, 5349–5357.

[48] Barboza JA, Iwakuma T, Terzian T, El-Naggar AK, and Lozano G (2008). Mdm2 and Mdm4 loss regulates distinct p53 activities. *Mol Cancer Res* **6**, 947–954.

[49] Datta A, Nag A, Pan W, Hay N, Gartel AL, Colamonici O, Mori Y, and Raychaudhuri P (2004). Myc-ARF (alternate reading frame) interaction inhibits the functions of Myc. *J Biol Chem* **279**, 36698–36707.

[50] Amente S, Gargano B, Diolaiti D, Della Valle G, Lania L, and Majello B (2007). $p14^{ARF}$ interacts with N-Myc and inhibits its transcriptional activity. *FEBS Lett* **581**, 821–825.

[51] Qi Y, Gregory MA, Li Z, Brousal JP, West K, and Hann SR (2004). $p19^{ARF}$ directly and differentially controls the functions of c-Myc independently of p53. *Nature* **431**, 712–717.

[52] Liu G, Schwartz JA, and Brooks SC (2000). Estrogen receptor protects p53 from deactivation by human double minute-2. *Cancer Res* **60**, 1810–1814.

[53] Kinyamu HK and Archer TK (2003). Estrogen receptor–dependent proteasomal degradation of the glucocorticoid receptor is coupled to an increase in mdm2 protein expression. *Mol Cell Biol* **23**, 5867–5881.

[54] Saji S, Okumura N, Eguchi H, Nakashima S, Suzuki A, Toi M, Nozawa Y, and Hayashi S (2001). MDM2 enhances the function of estrogen receptor alpha in human breast cancer cells. *Biochem Biophys Res Commun* **281**, 259–265.

[55] Keshelava N, Seeger RC, Groshen S, and Reynolds CP (1998). Drug resistance patterns of human neuroblastoma cell lines derived from patients at different phases of therapy. *Cancer Res* **58**, 5396–5405.

[56] Eischen CM, Weber JD, Roussel MF, Sherr CJ, and Cleveland JL (1999). Disruption of the ARF-Mdm2-p53 tumor suppressor pathway in Myc-induced lymphomagenesis. *Genes Dev* **13**, 2658–2669.

[57] Alt JR, Greiner TC, Cleveland JL, and Eischen CM (2003). Mdm2 haploinsufficiency profoundly inhibits Myc-induced lymphomagenesis. *EMBO J* **22**, 1442–1450.

[58] Eischen CM, Alt JR, and Wang P (2004). Loss of one allele of ARF rescues Mdm2 haploinsufficiency effects on apoptosis and lymphoma development. *Oncogene* **23**, 8931–8940.

[59] Wang P, Lushnikova T, Odvody J, Greiner TC, Jones SN, and Eischen CM (2008). Elevated Mdm2 expression induces chromosomal instability and confers a survival and growth advantage to B cells. *Oncogene* **27**, 1590–1598.

[60] Perfumo C, Parodi S, Mazzocco K, Defferrari R, Inga A, Haupt R, Fronza G, and Tonini GP (2008). Impact of MDM2 SNP309 genotype on progression and survival of stage 4 neuroblastoma. *Eur J Cancer* **44**, 2634–2639.

[61] Cattelani S, Defferrari R, Marsilio S, Bussolari R, Candini O, Corradini F, Ferrari-Amorotti G, Guerzoni C, Pecorari L, Menin C, et al. (2008). Impact of a single nucleotide polymorphism in the *MDM2* gene on neuroblastoma development and aggressiveness: results of a pilot study on 239 patients. *Clin Cancer Res* **14**, 3248–3253.

[62] Bond GL, Hu W, Bond EE, Robins H, Lutzker SG, Arva NC, Bargonetti J, Bartel F, Taubert H, Wuerl P, et al. (2004). A single nucleotide polymorphism in the MDM2 promoter attenuates the p53 tumor suppressor pathway and accelerates tumor formation in humans. *Cell* **119**, 591–602.